

Surfactant-Modified Nanoclay Exhibits an Antiviral Activity with High Potency and Broad Spectrum

Jian-Jong Liang,^a Jiun-Chiou Wei,^b Yi-Ling Lee,^a Shan-hui Hsu,^b Jiang-Jen Lin,^b Yi-Ling Lin^{a,c}

Institute of Biomedical Sciences^a and Genomics Research Center,^c Academia Sinica, Taipei, Taiwan; Institute of Polymer Science and Engineering, National Taiwan University, Taipei, Taiwan^b

ABSTRACT

Nanomaterials have the characteristics associated with high surface-to-volume ratios and have been explored for their antiviral activity. Despite some success, cytotoxicity has been an issue in nanomaterial-based antiviral strategies. We previously developed a novel method to fully exfoliate montmorillonite clay to generate the most fundamental units of nanoscale silicate platelet (NSP). We further modified NSP by capping with various surfactants and found that the surfactant-modified NSP (NSQ) was less cytotoxic. In this study, we tested the antiviral potentials of a series of natural-clay-derived nanomaterials. Among the derivatives, NSP modified with anionic sodium dodecyl sulfate (NSQc), but not the pristine clay, unmodified NSP, a silver nanoparticle-NSP hybrid, NSP modified with cationic *n*-octadecylamine hydrochloride salt, or NSP modified with nonionic Triton X-100, significantly suppressed the plaque-forming ability of Japanese encephalitis virus (JEV) at noncytotoxic concentrations. NSQc also blocked infection with dengue virus (DEN) and influenza A virus. Regarding the antiviral mechanism, NSQc interfered with viral binding through electrostatic interaction, since its antiviral activity can be neutralized by Polybrene, a cationic polymer. Furthermore, NSQc reduced the lethality of JEV and DEN infection in mouse challenge models. Thus, the surfactant-modified exfoliated nanoclay NSQc may be a novel nanomaterial with broad and potent antiviral activity.

IMPORTANCE

Nanomaterials have been investigated as antimicrobial agents, yet their antiviral potential is overshadowed by their cytotoxicity. By using a novel method, we fully exfoliated montmorillonite clay to generate the most fundamental units of nanoscale silicate platelet (NSP). Here, we show that the surfactant-modified NSP (NSQ) is less cytotoxic and that NSQc (NSP modified with sodium dodecyl sulfate) could potentially block infection by dengue virus (DEN), Japanese encephalitis virus (JEV), and influenza A virus at noncytotoxic concentrations. For the antiviral mechanism, we find that the electrostatic interaction between the negatively charged NSQc and the positively charged virus particles blocks viral binding. Furthermore, we used mouse challenge models of JEV and DEN to demonstrate the *in vivo* antiviral potential of NSQc. Thus, NSQc may function as a potent and safe antiviral nanohybrid against several viruses, and our success in synthesizing surfactant-modified NSP with antiviral activity may shed some light on future antiviral development.

Emerging viral infections have been threatening public health constantly; examples include the severe acute respiratory syndrome (SARS) coronavirus outbreak ~10 years ago and the recent H7N9 avian influenza A virus infection (1). Mosquito-borne flaviviruses, such as dengue virus (DEN) and Japanese encephalitis virus (JEV), are reemerging and affecting humans living in tropical and subtropical areas. DEN infection in humans causes a wide spectrum of illnesses ranging from mild dengue fever to severe complications such as dengue hemorrhagic fever and dengue shock syndrome (2, 3). JEV is the most important agent of viral encephalitis and causes acute encephalitis with high mortality in Asia (4). Inactivated and attenuated vaccines are available for JEV, but no vaccine exists for DEN, in part because of the complexity of the 4 serotypes of DEN and the potential involvement of antibody-dependent enhancement in severe dengue diseases. So far, no specific antiviral therapeutics are available for treating JEV and DEN infection (5, 6); thus, there is a great need to explore novel technology such as nanomaterials for their antiviral potential against these viruses.

Nanomaterials have the characteristics associated with high surface-to-volume ratios and generally exhibit unique properties not occurring in their micrometer-size analogs. The novel properties due to miniaturization of bulk materials have been inten-

sively exploited in many research fields, and the practical applications are numerous (7). The concept of creating nanosize pharmaceuticals has been explored for treating and preventing human diseases (8, 9). For example, high potencies of silver nanoparticles (AgNP) for antibacterial and antifungal activities have been well demonstrated (10). Continuing research on incorporating AgNP into a wide range of medical devices such as bone cement, surgical instruments, and wound dressings is being actively pursued. Recently, the antiviral effects of AgNP have been demonstrated against several viruses (10), such as HIV (11), herpes simplex virus (12), hepatitis B virus (13), respiratory syncytial virus (14), and influenza virus (15). However, the adverse effects of using nanoparticles such as AgNP, which have been found to be

Received 5 November 2013 Accepted 21 January 2014

Published ahead of print 29 January 2014

Editor: M. S. Diamond

Address correspondence to Yi-Ling Lin, yll@ibms.sinica.edu.tw, or Shan-hui Hsu, shhsu@ntu.edu.tw.

Copyright © 2014, American Society for Microbiology. All Rights Reserved.

doi:10.1128/JVI.03256-13

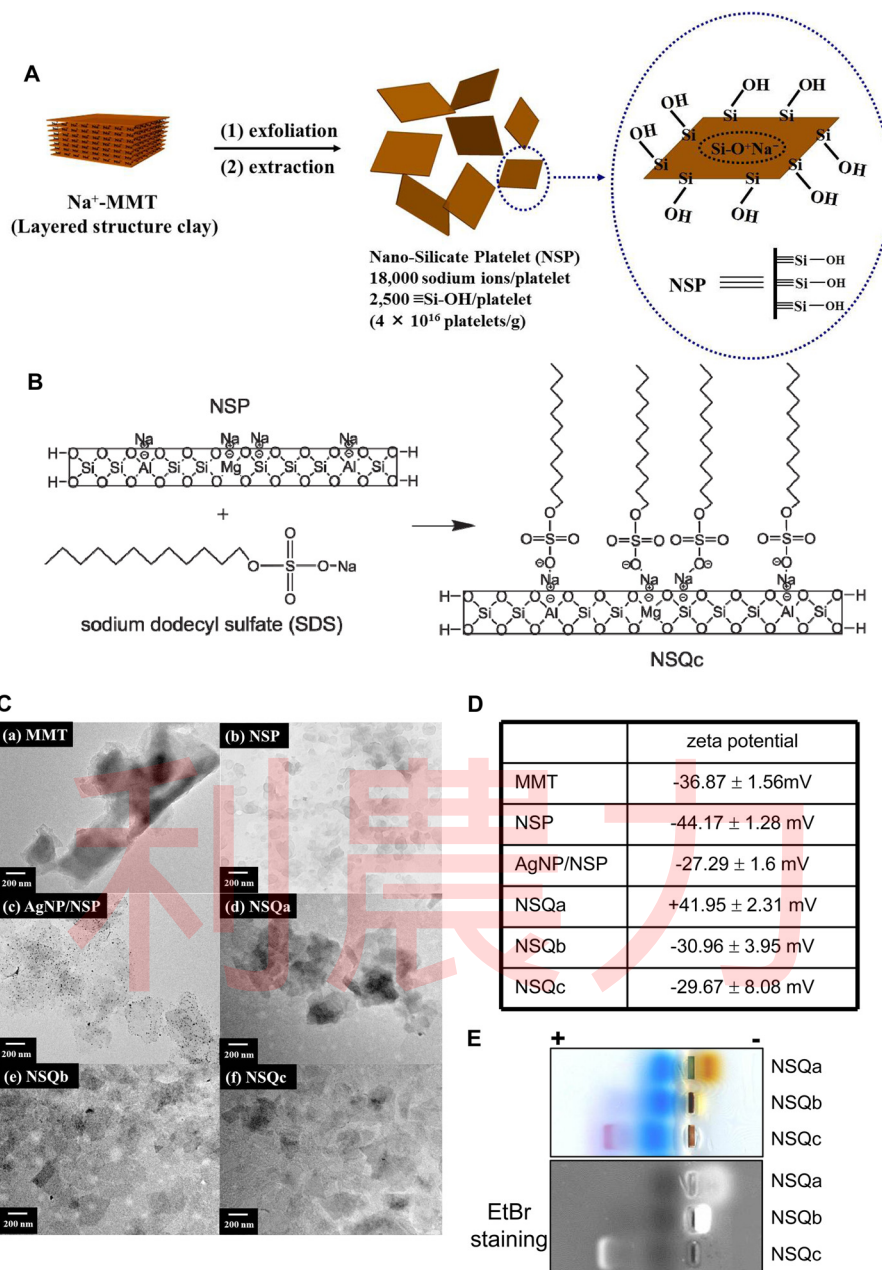


FIG 1 Characterization of the nanomaterials. (A and B) Conceptual illustrations of NSP (A) and SDS-modified NSQc (B). (C) Transmission electron micrographs of pristine MMT, NSP, AgNP/NSP, NSQa, NSQb, and NSQc. (D) Zeta potentials of the nanomaterials used in this study. (E) Agarose gel electrophoresis of NSQa, NSQb, and NSQc.

highly cytotoxic to many mammalian cells (10, 16, 17), are a concern, and applications of nanomaterials as antiviral agents have lagged behind similar antibacterial studies.

Naturally occurring clays such as montmorillonite (MMT) are conventionally used for catalysts and adsorbent agents and have been used as natural medicine (18–20). We developed a novel method to fully exfoliate MMT layered silicate clay to generate the most fundamental units of nanoscale silicate platelet (NSP) (21) (Fig. 1A), which possess higher antibacterial activity than the parental MMT in stack structure (22). The high surface-to-volume ratio and polyvalent anionic charges on a single platelet render

intense forces for 2-dimensional noncovalent bonding attraction and provide an extensive reacting surface for hybridizing AgNP on 1-nm-thick NSP. Synthesized AgNP/NSP nanohybrids inhibited the growth of several bacterial pathogens and even Ag-resistant *Escherichia coli* and drug-resistant *Staphylococcus aureus* (23, 24). Recently, we also found that AgNP/NSP protected chicks against salmonella infection (25). However, NSP with polyvalent ions could directly interact with the cell membrane, thus leading to some cytotoxic effects. To reduce the cytotoxicity, NSP was modified by capping with surfactants, because surfactant-capped nanomaterials are known to have lower cytotoxicity in general

(26). NSP was modified by the cationic *n*-octadecylamine hydrochloride salt (Qa), nonionic Triton X-100 (Qb), or anionic sodium dodecyl sulfate (SDS) (Qc) (27) (Fig. 1B). The surfactant-modified NSPs such as NSQa, NSQb, and NSQc commonly showed less cytotoxicity and enhanced antimicrobial activities, probably due to improvement of dispersibility in water (27).

In this study, we evaluated the antiviral potentials of a series of clay MMT-derived nanomaterials and found that NSQc, but not the pristine clay, unmodified NSP, AgNP/NSP, NSQa, or NSQb, potentially blocked the plaque-forming ability of JEV and also suppressed infection with DEN serotype 2 (DEN-2) and influenza A virus. The antiviral potency of NSQc depends on the composition of NSP and the surfactant SDS, because NSQc(A30), with a higher ratio of surfactant to NSP (70:30 weight ratio), showed stronger antiviral activity than NSQc(A50) (50:50 weight ratio). For the antiviral mechanism, we demonstrated an electrostatic interaction between the negatively charged NSQc and the positively charged virus particles as the predominant factor in antiviral action. Furthermore, we used mouse models of JEV and DEN infection to demonstrate the *in vivo* antiviral potential of NSQc. Thus, the complexes of NSP and negatively charged surfactant may be potent and safe antiviral nanomaterials against several pathogenic viruses.

MATERIALS AND METHODS

Cell lines and viruses. Baby hamster kidney fibroblast BHK-21 cells, human neuroblastoma SK-N-SH cells (ATCC HTB-11), and human lung carcinoma A549 cells were cultured as described previously (28, 29). The propagation and plaque formation of the JEV RP-9 strain and DEN-2 PL046 and NGC-N strains have been described previously (28, 29). Influenza A virus (H1N1, WSN) and MDCK (Madin-Darby canine kidney) cells were kindly provided by Michael Lai (Institute of Molecular Biology, Academia Sinica, Taipei, Taiwan).

Chemicals and antibodies. Hexadimethrine bromide (Polybrene) was from Sigma-Aldrich. Mouse antibodies against actin (Novus Biologicals), influenza A virus nucleoprotein (ab20343; Abcam), and JEV NS3 and DEN-2 NS3 proteins (30) were used.

NSQ preparation and characterization. NSP was isolated by one-step exfoliation of natural sodium MMT clay and toluene/aqueous NaOH extraction (21, 22). Three types of NSQ (NSQa, NSQb, and NSQc) were created by use of different surfactants with NSP as described previously (27). To remove the free SDS, NSQc was dialyzed against double-distilled water by use of a dialysis membrane (molecular weight cutoff [MWCO], 3,500; Membrane Filtration Products, Inc.) for 3 days. The mass percentages of NSP and SDS were obtained with a thermogravimetric analyzer (TGA 7; Perkin-Elmer, USA) at a heating rate of 10°C per min from 100 to 750°C. Nanomaterials were examined by using a transmission electron microscope (Hitachi H-7100) operated at 100 kV. The zeta potentials of nanomaterials in water were determined by laser light scattering using a zeta potential and submicrometer particle analyzer (Delsa Nano S; Beckman Coulter). For gel electrophoresis, the nanomaterials were mixed with loading dye (5% glycerol, 0.05% bromophenol blue, 0.05% xylene cyanol, and 0.05% neutral red) and separated on a 1% agarose gel in 0.5× Tris-borate-EDTA (TBE) buffer for 10 to 15 min at a constant voltage of 100 V. The gel was stained with ethidium bromide (EtBr) and photographed under UV light.

Cytotoxicity test. Cytotoxicity was assessed by use of the Cell Proliferation Kit II (XTT) (Roche). Briefly, BHK-21 cells (1×10^4 /well) were seeded in 96-well plates, incubated with the indicated compound (0 to 80 µg/ml) for 2 h, washed, and then cultured in fresh medium for 24 h. XTT labeling mixture was added and left for 1 to 2 h at 37°C before measurement of spectrophotometric absorbance with a microplate reader.

Antiviral tests in cells. For plaque reduction assay, BHK-21 cells seeded in 6-well plates were adsorbed with JEV (~200 PFU) mixed with the indicated compounds at room temperature for 1 h. After 2 h of viral adsorption, the virus and compounds were washed away and cells were overlaid with agarose-containing medium and incubated for 4 days. The plaques were fixed and stained with crystal violet solution (28). To determine the step of viral infection affected by NSQc, cells were treated with NSQc before virus adsorption for 2 h, during virus adsorption for 2 h, after virus adsorption for 22 h, or during all of these times for 26 h. After virus adsorption with a multiplicity of infection (MOI) of 5, cells were washed and incubated for 22 h at 37°C. Culture supernatants were collected for virus titration by plaque-forming assay, and cell lysates were harvested for Western blot analysis of viral protein expression (28). For virus binding assay, JEV (MOI of 1) was preincubated with 1 or 10 µg/ml of the indicated nanocompounds or phosphate-buffered saline (PBS) for 1 h at room temperature. Cells were adsorbed with the virus mixture for 2 h at 4°C and then were washed three times with cold serum-free medium. Total RNA was extracted with an RNeasy kit (Qiagen) and analyzed by real-time reverse transcription-PCR (RT-PCR) as previously described (31).

Mouse challenge assays. *Stat1*-deficient (*Stat1*^{-/-}) mice (32) and wild-type C57BL/6 mice were bred in the animal facility of the Institute of Biomedical Sciences, Academia Sinica (Taipei, Taiwan). The mouse experiments were approved and performed in accordance with the guidelines of the Academia Sinica Institutional Animal Care and Utilization Committee. To test whether NSQc treatment abolished the *in vivo* viral infectivity, JEV (RP-9; 2×10^5 PFU/mouse) and DEN-2 (NGC-N; 1×10^5 PFU/mouse) were incubated with NSQc (10 and 20 µg/ml) or PBS at 37°C for 2 h. Groups of 5-week-old mice were intraperitoneally (i.p.) inoculated with virus and intracerebrally (i.c.) injected with 30 µl of PBS (i.p. plus i.c. route) (33, 34). For the therapeutic mode of testing, groups of 5-week-old C57BL/6 mice were infected with JEV through the i.p. plus i.c. route, and then at 6 h postinfection, the mice were treated with the indicated NSQc compounds (20 or 80 µg/ml) or PBS by i.p. injection. The treatments were repeated at days 1, 2, 3, 5, 7, 9, 11, 13, and 15 postinfection. The mice were monitored daily for lethality. Relative JEV RNA levels in the brain tissues of mice therapeutically treated with the indicated NSQc compounds were determined by reverse transcription-quantitative PCR (RT-qPCR) as previously described (35) on day 5 postinfection. To test the effect of NSQc on naive mice, serum was collected at day 0, 5, and 25 after i.p. inoculation with 80 µg/ml NSQc, and the alanine aminotransferase (ALT) activity was determined by using Fuji Dri-Chem Slide GPT/ALT-P III (Fujifilm Corporation).

Statistical analysis. The 50% inhibitory concentration (IC₅₀), defined as the concentration inhibiting 50% of plaque formation, was determined by the modified Karber formulation. The 50% cytotoxic concentration (CC₅₀) was determined by linear regression analysis. For statistical comparisons between 2 groups of data, the two-tailed Student *t* test was used. Prism software with the log rank test was used to compare mouse survival curves.

RESULTS

Characterization of the nanomaterials. As examined by transmission electron microscopy, the exfoliated platelets of NSP were homogeneously present in water (Fig. 1C, panel b), in contrast to the aggregated lumps of MMT (Fig. 1C, panel a). In the case of AgNP/NSP, both Ag particles and silicate platelets were vividly observed (Fig. 1C, panel c). The images of NSP were slightly different from those of NSQa, NSQb, and NSQc (Fig. 1C, panels d to f), probably due to the different affinities between the neighboring platelets and the presence of surfactant molecules. For the ionic behaviors, the modified clays were analyzed for their zeta potentials. MMT and NSP demonstrated zeta potentials at steady values of -37 and -44 mV, respectively (Fig. 1D). With the addition of

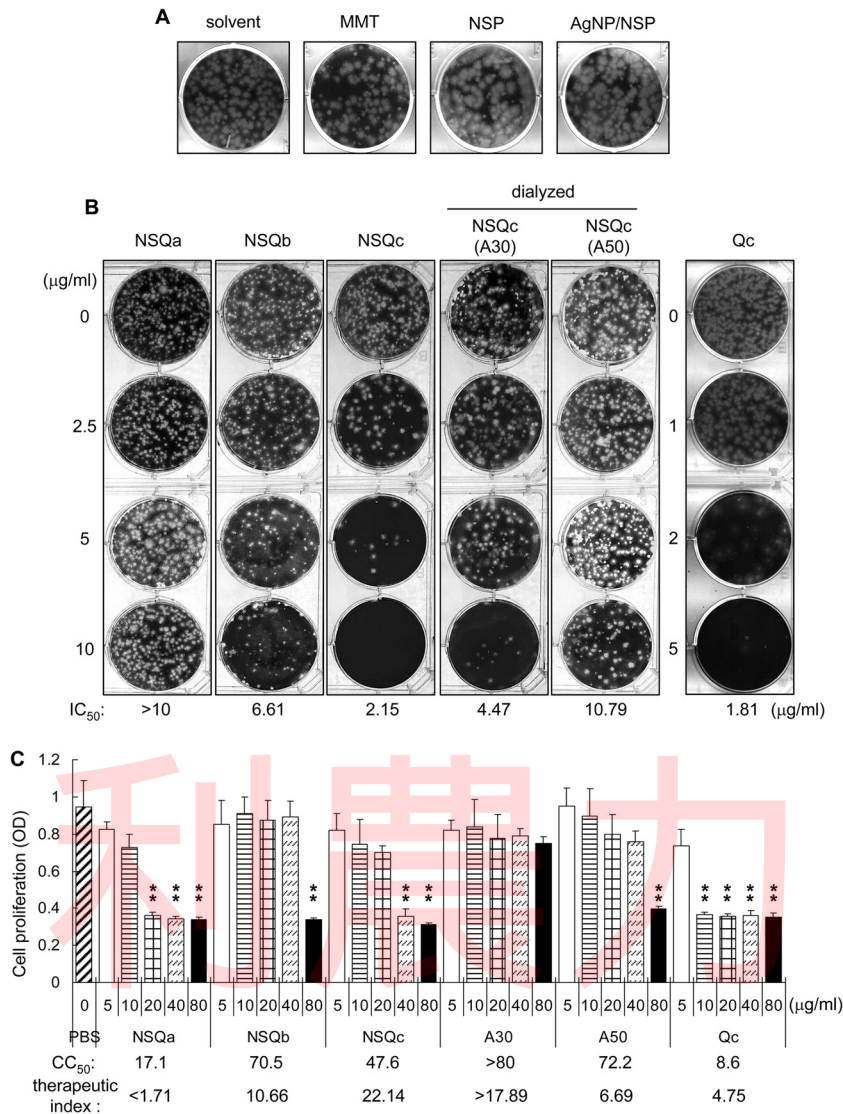


FIG 2 Potent anti-JEV effect of NSQc. (A and B) BHK-21 cells seeded in 6-well plates were adsorbed with JEV (~200 PFU) mixed with solvent (PBS) or 10 µg/ml MMT, NSP, or AgNP/NSP (A) or with the indicated NSQ compounds (0, 2.5, 5, and 10 µg/ml) or Qc (SDS) (0, 1, 2, and 5 µg/ml) (B). After 2 h of viral adsorption, cells were washed and overlaid with agarose-containing medium. Plaques were stained after 4 days of incubation with crystal violet solution. NSQc(A30) contained 30% NSP and 70% surfactant. NSQc(A50) contained 50% NSP and 50% surfactant. IC₅₀, concentration inhibiting 50% of plaque formation, calculated by the modified Karber formulation. (C) Cytotoxicity test of NSQ. BHK-21 cells were incubated with the indicated NSQ compounds at 5, 10, 20, 40, and 80 µg/ml, and cell growth was measured by XTT assay. The 50% cytotoxic concentration (CC₅₀) and therapeutic index (CC₅₀/IC₅₀) are shown at the bottom. Data are means ± standard deviations (SD) (*n* = 3). **, *P* < 0.01 compared with PBS control by Student's *t* test.

cationic surfactant to NSP, the zeta potential of NSQa greatly shifted to +42 mV, while modifications with AgNP, nonionic surfactant, and anionic surfactant resulted in only slight changes of the zeta potential for AgNP/NSP, NSQb, and NSQc (Fig. 1D). The charge modification was confirmed by agarose gel electrophoresis, as NSQc with modification of negatively charged surfactant migrated toward the anode (Fig. 1E). These results provide evidence showing the characteristic changes of NSP with different modifications.

Potent anti-JEV effect of NSQc. We used plaque formation assays to evaluate the antiviral potentials of a series of clay MMT-derived nanomaterials against JEV infection. The plaque numbers and sizes were similar with the solvent control and treatment with 10 µg/ml of MMT, NSP, or AgNP/NSP (Fig. 2A). NSQa, which is

NSP modified with cationic *n*-octadecylamine hydrochloride salt, had no effect on JEV infection at 10 µg/ml (Fig. 2B). NSQb, which is NSP modified with nonionic Triton X-100, slightly reduced JEV infection, with an IC₅₀ of 6.61 µg/ml (Fig. 2B). Interestingly, NSQc, which is NSP modified with anionic SDS, greatly blocked JEV infection, as 10 µg/ml of NSQc completely eliminated the plaque-forming ability of JEV (IC₅₀ = 2.15 µg/ml) (Fig. 2B).

To address whether some of the surfactant SDS might be dissociated from NSP in NSQc solution, we used thermogravimetric analysis to measure the mass percentages of NSP and SDS before and after dialysis. The undialyzed NSQc contains 42% NSP and 58% SDS (despite the fact that it is 30% NSP and 70% SDS during synthesis), and 71% of the SDS was NSP bound and the remaining

29% was free in solution. To exclude the possibility that the antiviral activity of NSQc is derived from the free surfactant SDS, which had a potent anti-JEV activity (IC_{50} of 1.81 $\mu\text{g/ml}$) (Fig. 2B), we used the dialyzed NSQc [designated NSQc(A30) to distinguish it from the undialyzed NSQc], whose free SDS was completely removed, in a JEV plaque reduction assay. NSQc(A30) was still able to reduce more than 90% of plaque formation at 10 $\mu\text{g/ml}$ (Fig. 2B), indicating that the antiviral activity of NSQc was not solely contributed by the free SDS in solution. To address whether the amounts of surfactant on NSP affect the antiviral activity, we tested the antiviral potential of NSQc(A50) [50% NSP and 50% surfactant, while NSQc(A30) has a ratio of 30% NSP to 70% surfactant]. The antiviral activity of NSQc(A30) was greater than that of NSQc(A50), with IC_{50} s of 4.47 $\mu\text{g/ml}$ and 10.79 $\mu\text{g/ml}$, respectively (Fig. 2B). Thus, NSQc with a higher ratio of surfactant to NSP has stronger anti-JEV activity.

Importantly, the antiviral activity of NSQc did not result from a cytotoxic effect on host cells, because cell proliferation measured by XTT assays showed that at 10 $\mu\text{g/ml}$, all types of NSQ did not affect cell growth, in contrast to SDS, which had high cytotoxicity at 10 $\mu\text{g/ml}$ (Fig. 2C). After dialysis to remove the free surfactant, NSQc(A30) had lower cytotoxicity than the parental NSQc, as 80 $\mu\text{g/ml}$ NSQc(A30) had no significant effect on cell growth (Fig. 2C). Overall, NSQc and NSQc(A30) have the best therapeutic indices (CC_{50}/IC_{50}) of 22.14 and >17.89 , respectively, whereas the others were either not potent enough or too toxic. Thus, among the 6 clay-derived nanomaterials tested, NSQc was a safe and potent anti-JEV agent.

NSQc blocks early steps of JEV infection. To determine the steps of JEV infection blocked by NSQc, we used 4 different protocols of treatment: NSQc was added to cells before virus adsorption for 2 h, during virus adsorption for 2 h, after virus adsorption for 22 h, and during all of these times for 26 h. JEV infection of HTB-11 cells, a human neuroblastoma cell line, was blocked by only 2 modes of treatment (during virus adsorption and during all times) at 10 $\mu\text{g/ml}$, as determined by Western blot analysis of viral NS3 protein expression and plaque formation assays for viral progeny production (Fig. 3A and B). Similar results were noted for dialyzed NSQc(A30) (Fig. 3C and D). The fact that 2 h of treatment during viral adsorption had an antiviral effect similar to that of 26 h of treatment during all time periods strongly suggests that NSQc blocks JEV infection mainly at the early steps of viral infection.

NSQc relies on electrostatic interaction to inhibit virus binding. To test whether the first step of viral infection, binding to the cell surface, is affected by NSQc, we did a viral binding assay by incubating cells with the virus-NSQc mixture at 4°C. The amounts of virus bound on the cell surface were quantified by measuring the viral RNA with real-time RT-PCR. Preincubation of JEV with 10 $\mu\text{g/ml}$ of NSQc and NSQc(A30), but not with NSQc(A50), reduced 70 to 80% of JEV binding onto cell surface (Fig. 4A). Our data thus suggest that NSQc is able to block JEV binding. Regarding the antiviral mechanism, we used Polybrene, a cationic polymer, to evaluate whether the negative charge of NSQc is responsible for its antiviral action. Preincubating NSQc(A30) with Polybrene greatly abolished the anti-JEV activity of NSQc(A30) (Fig. 4B and C), indicating that the negative charge of NSQc is essential for its antiviral activity. We then used dimethyl sulfoxide (DMSO), an organic solvent that dissolves hydrophobic compounds, to test whether the hydrophobic region of NSQc is re-

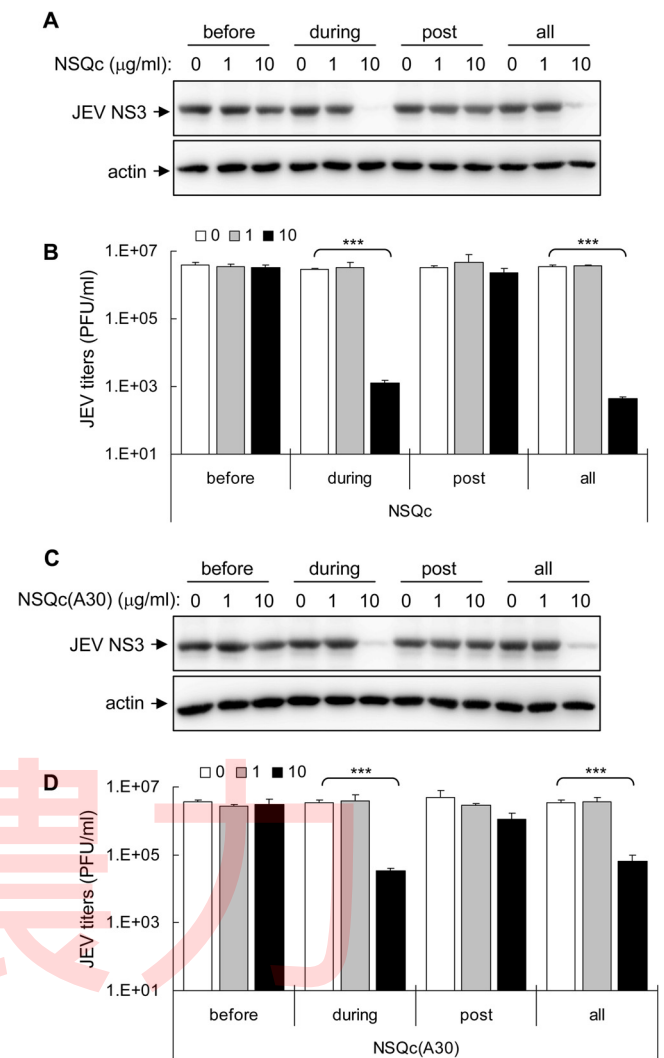


FIG 3 JEV viral entry is blocked by NSQc. Human neuronal HTB-11 cells were treated with 0, 1, and 10 $\mu\text{g/ml}$ NSQc (A and B) or NSQc(A30) (C and D) before virus adsorption for 2 h (before), during virus adsorption for 2 h (during), after virus adsorption for 22 h (post), or during all of these times for 26 h (all). Western blot analysis was performed for protein levels of JEV NS3 and actin as a loading control in cell lysates. The virus titers (PFU/ml) are means \pm SD ($n = 3$). The titers of the indicated groups were compared using Student's t test. ***, $P < 0.001$.

sponsible for its antiviral action. Preincubation with DMSO (0.2% and 1%) did not abolish the anti-JEV activity of NSQc and NSQc(A30) (Fig. 4D and E), indicating that the hydrophobic region of NSQc may not play a major role in its antiviral activity.

NSQc suppresses infection by DEN-2 and influenza A virus. To explore the antiviral spectrum of NSQc, we determined the antiviral potentials of NSQc on another flavivirus, DEN-2, and influenza A virus, an orthomyxovirus. NSQc and NSQc(A30) (10 $\mu\text{g/ml}$) added during viral adsorption reduced the viral protein expression and virus production by DEN-2 as determined by Western blot analysis of viral NS3 protein and plaque formation assay (Fig. 5A) and those of influenza A virus as determined by Western blot analysis of influenza virus nucleoprotein (NP) and plaque formation assay (Fig. 5B). Similar to the results for JEV, antiviral activity against DEN-2 and influenza virus was lower

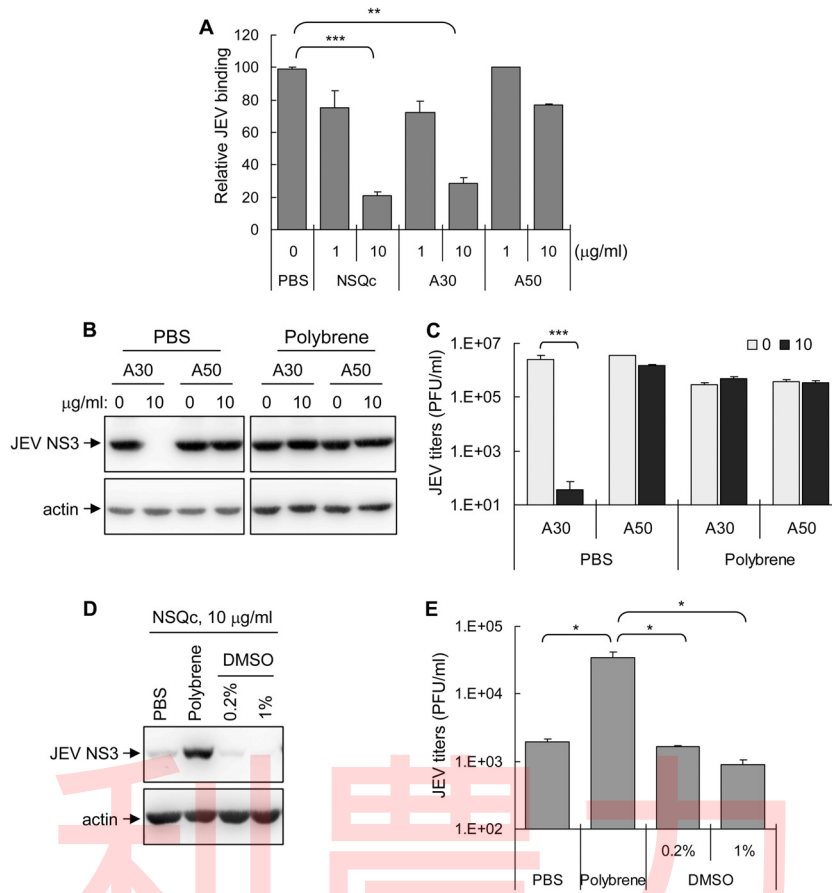


FIG 4 NSQc and NSQc(A30) reduce JEV binding on the cell surface through electrostatic interaction. (A) JEV preincubated with the indicated NSQc (1 and 10 $\mu\text{g/ml}$) at room temperature for 1 h was adsorbed onto BHK-21 cells at 4°C for 2 h. After extensive washing, the cells were collected for RNA extraction and the amounts of cell surface-associated virus were quantified by real-time RT-PCR. The JEV RNA copy numbers were normalized to that of actin. The amounts of JEV binding relatively to the PBS control were calculated and are shown. Data are means \pm SD ($n = 3$) and were compared using Student's t test. **, $P < 0.01$; ***, $P < 0.001$. (B) NSQc(A30) and NSQc(A50) (0 and 10 $\mu\text{g/ml}$) were incubated with PBS or Polybrene (5 $\mu\text{g/ml}$) for 1 h, and then JEV was added and left for another 1 h. HTB-11 cells adsorbed with these mixtures for 2 h (MOI of 5) were washed and incubated at 37°C for 22 h. Western blot analysis of protein levels of JEV NS3 and actin in cell lysates was performed. (C) The virus titers (PFU/ml) are means \pm SD ($n = 3$), and the indicated groups were compared using Student's t test. **, $P < 0.01$; ***, $P < 0.001$. (D) NSQc (10 $\mu\text{g/ml}$) was incubated with PBS, Polybrene (5 $\mu\text{g/ml}$), or DMSO (0.2% and 1%) for 1 h, and then JEV was added and left for another 1 h. BHK-21 cells adsorbed with these mixtures for 2 h (MOI of 1) were washed and incubated at 37°C for 22 h. Western blot analysis of protein levels of JEV NS3 and actin in cell lysates was performed. (E) The virus titers (PFU/ml) are means \pm SD ($n = 3$), and the indicated groups were compared using Student's t test. *, $P < 0.05$.

with NSQc(A50) than with NSQc and NSQc(A30). Furthermore, preincubating NSQc(A30) with Polybrene greatly abolished its anti-DEN-2 and anti-influenza virus activities (Fig. 5C and D). Thus, depending on the amount of surfactant and negative charge, NSQc had antiviral activity against several viruses.

NSQc alleviates the mortality of mice infected with JEV and DEN-2. JEV is a neurotropic virus and causes acute encephalitis in humans. Mice have been the most commonly used and thoroughly characterized animal model for JEV infection (36). In our established murine model (28, 37), mice infected with a virulent JEV strain RP-9 can show signs of ruffled fur, hunchback, limb weakness, and paralysis, and they die at approximately 10 days postinfection. Developing an adequate mouse model for DEN has been more difficult, since wild-type mice are resistant to DEN-induced diseases (38). We have developed a DEN model in *Stat1*^{-/-} mice, which showed paralysis, hemorrhage, vascular leakage, and death after being challenged with a mouse-adapted

DEN strain (39). Here, we used the established murine models of JEV (28, 37) and DEN-2 (39) to assess whether NSQc treatment can impede the *in vivo* viral infectivity. In C57BL/6 mice, infection with JEV killed 80% of the inoculated mice (Fig. 6A), whereas all mice survived infection with JEV preincubated with NSQc (10 and 20 $\mu\text{g/ml}$) or NSQc(A30) (20 $\mu\text{g/ml}$). The less competent NSQc(A50) at 20 $\mu\text{g/ml}$ also protected 80% of mice against JEV challenge (Fig. 6A). For DEN-2 infection, all of the *Stat1*^{-/-} mice died upon challenge with DEN-2, whereas preincubation of DEN-2 with 20 $\mu\text{g/ml}$ of NSQc, NSQc(A30), or NSQc(A50) completely eliminated the ability of DEN-2 to kill mice (Fig. 6B). We further used a postchallenge treatment mode to evaluate the *in vivo* antiviral potential of NSQc. Starting from 6 h after JEV infection, treatment with NSQc or NSQc(A30) (80 $\mu\text{g/ml}$ per treatment) protected 60 to 80% of mice inoculated with JEV, whereas a lower dose of NSQc and NSQc(A30) (20 $\mu\text{g/ml}$), NSQc(A50) and the PBS control did not provide protection against JEV infec-

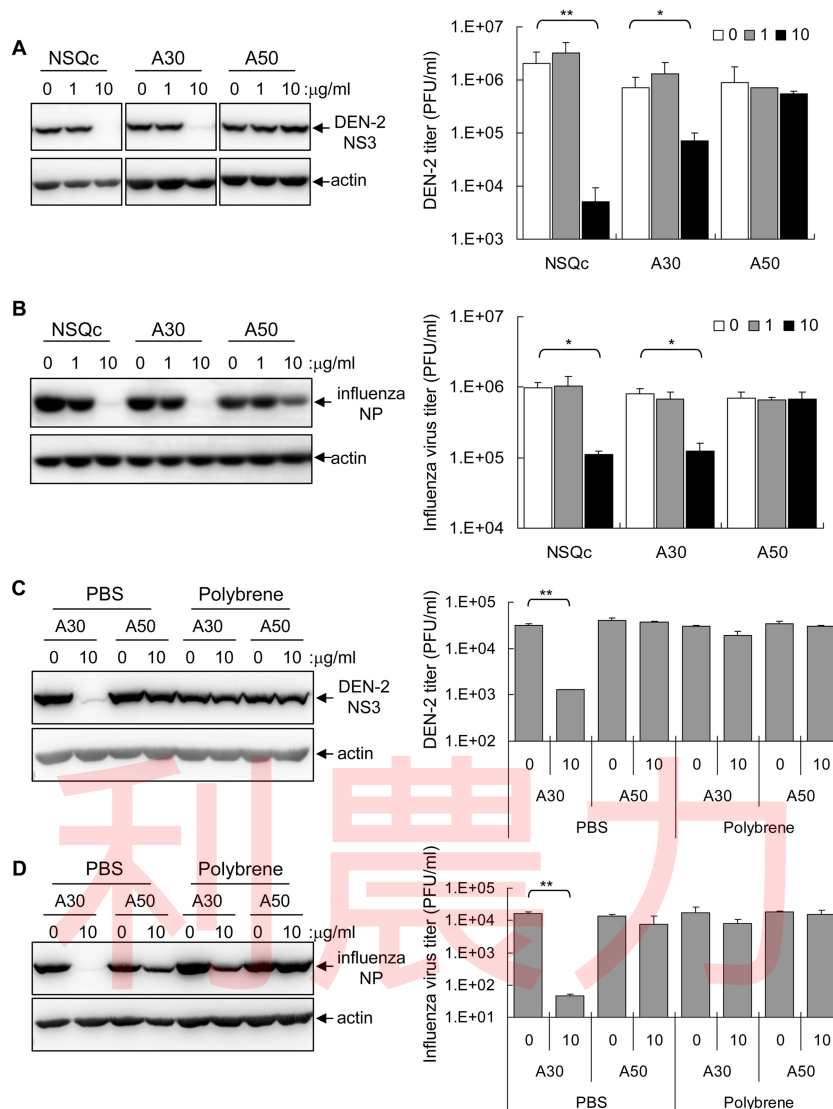


FIG 5 Antiviral spectrum of NSQc. (A and B) The indicated NSQc compounds (0, 1, and 10 µg/ml) were incubated with DEN-2 (A) or influenza A virus (B) for 1 h (MOI of 5). (C and D) For the antiviral blockage test, NSQc(A30) and NSQc(A50) (0 and 10 µg/ml) were incubated with PBS or Polybrene (5 µg/ml) for 1 h and then incubated with DEN-2 (C) or influenza A virus (D) for 1 h. The mixture of DEN-2 was adsorbed onto BHK-21 cells and that of influenza A virus onto A549 cells for 2 h (MOI of 0.1). After virus adsorption, cells were washed and further incubated at 37°C for 22 h. Western blot analysis of protein levels of DEN-2 NS3, influenza virus NP, and actin as a loading control was performed. The virus titers (PFU/ml) are means ± SD ($n = 3$), and the indicated groups were compared using Student's *t* test. *, $P < 0.05$; **, $P < 0.01$.

tion (Fig. 6C). Furthermore, the levels of viral replication in the brains of mice treated with 80 µg/ml NSQc or NSQc(A30) post-challenge (with a 6-h delay) were lower than those in mice treated with PBS or NSQc(A50) (Fig. 6D). However, further delay of the treatment to 1 day after JEV challenge did not confer a protective effect (data not shown), indicating that NSQc targets an early step of the viral life cycle and should be given early after infection. Whether NSQc could protect mice from challenge with other viral strains and by other routes of infection such as intravenous inoculation remains elusive. To address the potential adverse effect of NSQc, we measured the serum alanine aminotransferase (ALT) level, an indicator of liver injury, and no abnormality was noted in naive mice inoculated with a high dose of NSQc compounds (80 µg/ml) (Fig. 6E). Thus, NSQc is safe and may exhibit preventive

and therapeutic potential against viral infection in challenged mice.

DISCUSSION

The MMT-*exfoliated* NSP and AgNP/NSP nanohybrids have potent antibacterial activity (22, 24, 40), but under noncytotoxic conditions, NSP or even NSP coated with AgNP had no anti-JEV effect (Fig. 2A). By capping of surfactants, we generated 3 new types of NSQ that appeared to be less cytotoxic than the parental NSP (27). The cationic NSQa had no anti-JEV activity, in accordance with our notion that a negative charge of NSQ is required for its antiviral mechanism. The nonionic NSQb with a negative zeta potential exhibited a weak anti-JEV activity (Fig. 2B). The most potent antiviral activity was noted with NSQc, which is NSP

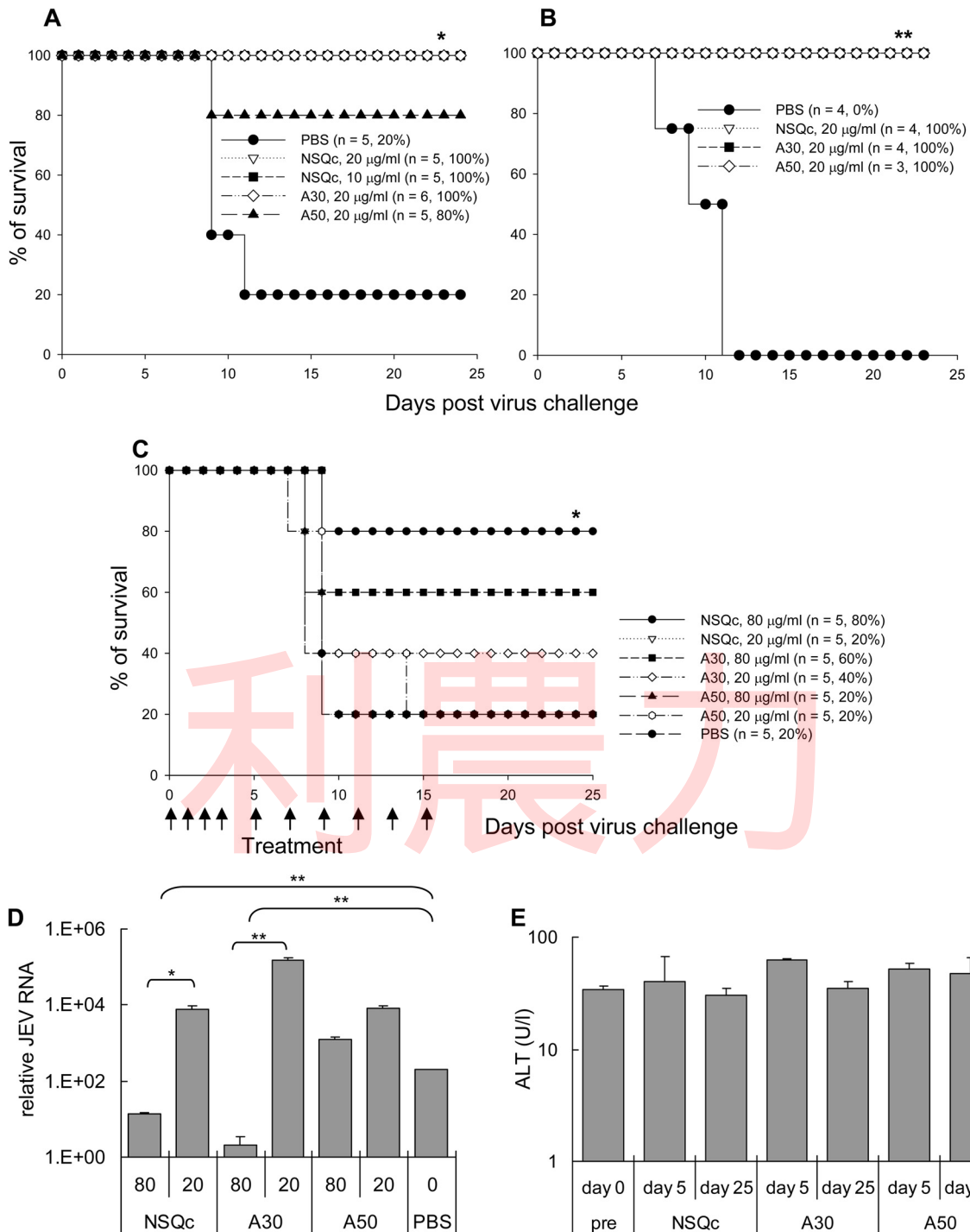


FIG 6 *In vivo* antiviral potential of NSQc. (A) C57BL/6 mice were challenged with JEV (RP-9; 2×10^5 PFU/mouse) preincubated with the indicated NSQc compounds (10 or 20 $\mu\text{g/ml}$) or PBS. (B) *Stat1*^{-/-} mice were infected with DEN-2 (NGC-N; 1×10^5 PFU/mouse) preincubated with the indicated NSQc compounds (20 $\mu\text{g/ml}$) or PBS. (C) C57BL/6 mice were challenged with JEV (RP-9; 2×10^5 PFU/mouse), and starting from 6 h postinfection, the mice were treated with the indicated NSQc compounds (20 or 80 $\mu\text{g/ml}$) or PBS at the indicated days postinfection (arrows). The survival of mice was observed daily. The numbers of mice in each group and the survival rates are shown in parentheses. Prism software with the log rank test was used to compare survival curves. *, $P < 0.05$; **, $P < 0.01$. (D) Mice that received treatment with the indicated NSQc after a 6-h delay were sacrificed at day 5, and the relative JEV RNA levels in the brain tissues were quantified by RT-qPCR and normalized to that of actin. (E) Naive C57BL/6 mice were i.p. inoculated with 80 $\mu\text{g/ml}$ NSQc, NSQc(A30), or NSQc(A50). Serum samples were collected at the indicated days, and their alanine aminotransferase (ALT) levels were determined.

modified with the anionic Qc (SDS). SDS has excellent antibacterial and antiviral activities (41). However, because of cytotoxicity and biomedical safety concerns (42), SDS is used in shampoos and toothpastes at low concentrations. Our ability to conjugate SDS to NSP as in NSQc greatly reduced the cytotoxicity and allowed for exploration of the *in vitro* and *in vivo* antiviral potentials. Our result that dialyzed NSQc still had potent antiviral activity indicates that the antiviral action of NSQc is not simply due to the free SDS. Thus, the combination of NSP and SDS, or perhaps other anionic surfactants, may pave a new way to develop novel antiviral nanomaterials.

In this study, we demonstrated the antiviral activities of NSQc against 3 different viruses, JEV, DEN, and influenza A virus, all of which are enveloped viruses. Because enveloped viruses can be inactivated by detergent treatment through hydrophobic interaction (43), the hydrophobic region of NSQc may be a lipid solvent inhibiting the enveloped viruses. However, the fact that positively charged Polybrene but not the organic solvent DMSO could neutralize the antiviral activity of NSQc (Fig. 4) argues against the mechanism of hydrophobic interaction. Another possible mode of antiviral action is through reactive oxygen species (ROS), since NSP and AgNP/NSP could disrupt bacterial membrane integrity through ROS generation (23, 24). We used sodium azide (NaN_3), a singlet-oxygen scavenger (44), to test whether ROS are involved in the antiviral mechanism of NSQc. Preincubation with 25 mM NaN_3 did not block the antiviral ability of NSQc (data not shown), suggesting that the generation of ROS may not play a role in viral inactivation with NSQc.

DEN and JEV are enveloped flaviviruses, which initiate viral infection by attachment of envelope proteins to cell surface receptors for entry into cells via receptor-mediated endocytosis (45). Highly sulfated glycosaminoglycans (GAGs) can bind JEV (46) and DEN (47), and negatively charged heparin interferes with viral attachment and blocks JEV and DEN infection. Influenza virus relies on sialic acid to infect cells (48, 49). GAGs are long unbranched polysaccharides consisting of a repeating disaccharide unit that consists of a hexose linked to a hexosamine. Sialic acid is a generic term for the N- or O-substituted derivatives of neuraminic acid. Our results showing that NSQc blocks infection with JEV/DEN and influenza A virus, which use different cell surface molecules to initiate infection, strongly suggest that NSQc may share a property of GAGs and sialic acid such as a negative charge. The negatively charged NSQc may trap virus by electrostatic interaction, prevent the interaction of virus and host cell, and then block viral binding/entry into the host cell (as outlined in Fig. 7). Thus, NSQc might also have antiviral activity against other related viruses such as West Nile virus, which has been endemic in the United States since 1999 (50), or even other unrelated viruses that rely on charge-charge interaction to interact with host cells.

With more than one-third of the world's population living in areas at risk for DEN transmission, DEN is a leading cause of illness and death in the tropics and subtropics. Currently, there is no DEN vaccine or specific medication for treating DEN infection. Despite the availability of JE vaccines, JEV is still the leading cause of viral encephalitis in Asia, with more than 50,000 cases and 10,000 deaths annually. Influenza virus is transmitted easily from person to person and causes seasonal epidemics around the world. Three influenza pandemics occurred in the 20th century and killed tens of millions of people. Antiviral drugs such as the neuraminidase inhibitor oseltamivir (Tamiflu) have been used to treat

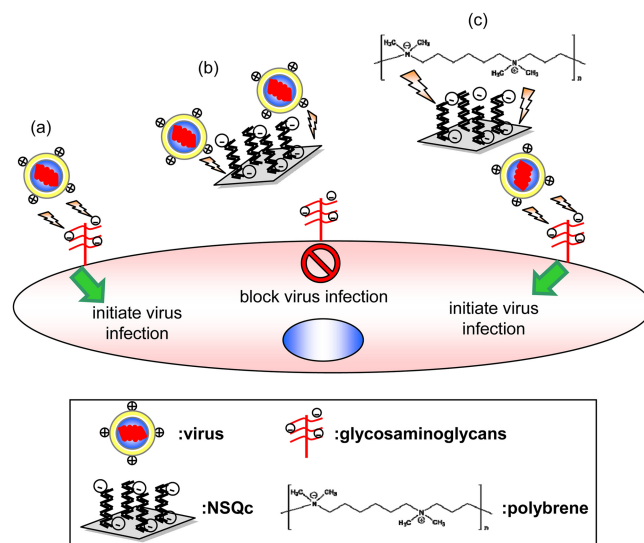


FIG 7 Possible mechanism of NSQc-mediated antiviral activity. The positively charged virus particles adsorb to cell surface by interacting with negatively charged molecules such as glycosaminoglycans to initiate virus infection (a). The negatively charged NSQc is able to adsorb with virus particles and then results in blocking of viral binding onto the host cell (b). Cationic material such as Polybrene neutralizes the negative charge of NSQc and prevents the blocking of virus by NSQc (c).

influenza; however, drug-resistant influenza virus strains and novel avian-origin influenza viruses are emerging (51). Therefore, antiviral agents against these devastating human pathogens are urgently needed. Our success in synthesizing surfactant-modified NSP and our finding that this novel NSQc nanocompound can block several viruses may shed some light on future antiviral development.

ACKNOWLEDGMENTS

We thank Michael Lai (Institute of Molecular Biology, Academia Sinica, Taiwan) for providing the influenza A virus H1N1 WSN strain.

This work was supported by the National Research Program for Nanoscience and Technology, sponsored by the National Science Council (NSC 100-2120-M-002-006), and by grants from Academia Sinica, Taiwan.

The authors declare that they have no conflict of interest.

REFERENCES

- Li Q, Zhou L, Zhou M, Chen Z, Li F, Wu H, Xiang N, Chen E, Tang F, Wang D, Meng L, Hong Z, Tu W, Cao Y, Li L, Ding F, Liu B, Wang M, Xie R, Gao R, Li X, Bai T, Zou S, He J, Hu J, Xu Y, Chai C, Wang S, Gao Y, Jin L, Zhang Y, Luo H, Yu H, Gao L, Pang X, Liu G, Shu Y, Yang W, Uyeki TM, Wang Y, Wu F, Feng Z. 24 April 2013. Preliminary report: epidemiology of the avian influenza A (H7N9) outbreak in China. *N. Engl. J. Med.* <http://dx.doi.org/10.1056/NEJMoa1304617>.
- Simmons CP, Farrar JJ, Nguyen VV, Wills B. 2012. Dengue. *N. Engl. J. Med.* 366:1423–1432. <http://dx.doi.org/10.1056/NEJMra1110265>.
- Guzman MG, Halstead SB, Artsob H, Buchy P, Farrar J, Gubler DJ, Hunsperger E, Kroeger A, Margolis HS, Martinez E, Nathan MB, Pelegrino JL, Simmons C, Yoksan S, Peeling RW. 2010. Dengue: a continuing global threat. *Nat. Rev. Microbiol.* 8:S7–16. <http://dx.doi.org/10.1038/nrmicro2460>.
- Solomon T. 2004. Flavivirus encephalitis. *N. Engl. J. Med.* 351:370–378. <http://dx.doi.org/10.1056/NEJMra030476>.
- Heinz FX, Stiasny K. 2012. Flaviviruses and flavivirus vaccines. *Vaccine* 30:4301–4306. <http://dx.doi.org/10.1016/j.vaccine.2011.09.114>.
- Sayce AC, Miller JL, Zitzmann N. 2010. Targeting a host process as an

- antiviral approach against dengue virus. *Trends Microbiol.* 18:323–330. <http://dx.doi.org/10.1016/j.tim.2010.04.003>.
7. Rivera Gil P, Huhn D, del Mercato LL, Sasse D, Parak WJ. 2010. Nanopharmacy: inorganic nanoscale devices as vectors and active compounds. *Pharmacol. Res.* 62:115–125. <http://dx.doi.org/10.1016/j.phrs.2010.01.009>.
 8. Jain KK. 2008. Nanomedicine: application of nanobiotechnology in medical practice. *Med. Princ. Pract.* 17:89–101. <http://dx.doi.org/10.1159/000112961>.
 9. Bawarski WE, Chidlowsky E, Bharali DJ, Mousa SA. 2008. Emerging nanopharmaceuticals. *Nanomedicine* 4:273–282. <http://dx.doi.org/10.1016/j.nano.2008.06.002>.
 10. Galdiero S, Falanga A, Vitiello M, Cantisani M, Marra V, Galdiero M. 2011. Silver nanoparticles as potential antiviral agents. *Molecules* 16: 8894–8918. <http://dx.doi.org/10.3390/molecules16108894>.
 11. Elechiguerra JL, Burt JL, Morones JR, Camacho-Bragado A, Gao X, Lara HH, Yacaman MJ. 2005. Interaction of silver nanoparticles with HIV-1. *J. Nanobiotechnol.* 3:6. <http://dx.doi.org/10.1186/1477-3155-3-6>.
 12. Baram-Pinto D, Shukla S, Perkas N, Gedanken A, Sarid R. 2009. Inhibition of herpes simplex virus type 1 infection by silver nanoparticles capped with mercaptoethane sulfonate. *Bioconjug. Chem.* 20:1497–1502. <http://dx.doi.org/10.1021/bc900215b>.
 13. Lu L, Sun RW, Chen R, Hui CK, Ho CM, Luk JM, Lau GK, Che CM. 2008. Silver nanoparticles inhibit hepatitis B virus replication. *Antivir. Ther.* 13:253–262.
 14. Sun L, Singh AK, Vig K, Pillai SR, Singh SR. 2008. Silver nanoparticles inhibit replication of respiratory syncytial virus. *J. Biomed. Nanotechnol.* 4:149–158. <http://dx.doi.org/10.1166/jbn.2008.012>.
 15. Xiang DX, Chen Q, Pang L, Zheng CL. 2011. Inhibitory effects of silver nanoparticles on H1N1 influenza A virus in vitro. *J. Virol. Methods* 178: 137–142. <http://dx.doi.org/10.1016/j.jviromet.2011.09.003>.
 16. Bae E, Park H, Park J, Yoon J, Kim Y, Choi K, Yi J. 2011. Effect of chemical stabilizers in silver nanoparticle suspensions on nanotoxicity. *Bull. Korean Chem. Soc.* 32:613–619. <http://dx.doi.org/10.5012/bkcs.2011.32.2.613>.
 17. Magaña SM, Quintana P, Aguilar DH, Toledo JA, Angeles-Chávez C, Cortés MA, León L, Freile-Pelegrín Y, López T, Sánchez RMT. 2008. Antibacterial activity of montmorillonites modified with silver. *J. Mol. Catal. A: Chem.* 281:192–199. <http://dx.doi.org/10.1016/j.molcata.2007.10.024>.
 18. Williams LB, Metge DW, Eberl DD, Harvey RW, Turner AG, Prapapong P, Poret-Peterson AT. 2011. What makes a natural clay antibacterial? *Environ. Sci. Technol.* 45:3768–3773. <http://dx.doi.org/10.1021/es1040688>.
 19. Haydel SE, Remenih CM, Williams LB. 2008. Broad-spectrum in vitro antibacterial activities of clay minerals against antibiotic-susceptible and antibiotic-resistant bacterial pathogens. *J. Antimicrob. Chemother.* 61: 353–361. <http://dx.doi.org/10.1093/jac/dkm468>.
 20. Pinnavaia TJ. 1983. Intercalated clay catalysts. *Science* 220:365–371. <http://dx.doi.org/10.1126/science.220.4595.365>.
 21. Lin JJ, Chu CC, Chiang ML, Tsai WC. 2006. First isolation of individual silicate platelets from clay exfoliation and their unique self-assembly into fibrous arrays. *J. Phys. Chem. B* 110:18115–18120. <http://dx.doi.org/10.1021/jp0636773>.
 22. Hsu SH, Tseng HJ, Hung HS, Wang MC, Hung CH, Li PR, Lin JJ. 2009. Antimicrobial activities and cellular responses to natural silicate clays and derivatives modified by cationic alkylamine salts. *ACS Appl. Mater. Interfaces* 1:2556–2564. <http://dx.doi.org/10.1021/am900479q>.
 23. Su HL, Chou CC, Hung DJ, Lin SH, Pao IC, Lin JH, Huang FL, Dong RX, Lin JJ. 2009. The disruption of bacterial membrane integrity through ROS generation induced by nanohybrids of silver and clay. *Biomaterials* 30:5979–5987. <http://dx.doi.org/10.1016/j.biomaterials.2009.07.030>.
 24. Su HL, Lin SH, Wei JC, Pao IC, Chiao SH, Huang CC, Lin SZ, Lin JJ. 2011. Novel nanohybrids of silver particles on clay platelets for inhibiting silver-resistant bacteria. *PLoS One* 6:e21125. <http://dx.doi.org/10.1371/journal.pone.0021125>.
 25. Chiao SH, Lin SH, Shen CI, Liao JW, Bau JJ, Wei JC, Tseng LP, Hsu SH, Lai PS, Lin SZ, Lin JJ, Su HL. 2012. Efficacy and safety of nanohybrids comprising silver nanoparticles and silicate clay for controlling *Salmonella* infection. *Int. J. Nanomed.* 7:2421–2432. <http://dx.doi.org/10.2147/IJN.S31594>.
 26. Teow Y, Asharani PV, Hande MP, Valiyaveetil S. 2011. Health impact and safety of engineered nanomaterials. *Chem. Commun. (Camb.)* 47: 7025–7038. <http://dx.doi.org/10.1039/c0cc05271j>.
 27. Wang MC, Lin JJ, Tseng HJ, Hsu SH. 2012. Characterization, antimicrobial activities, and biocompatibility of organically modified clays and their nanocomposites with polyurethane. *ACS Appl. Mater. Interfaces* 4:338–350. <http://dx.doi.org/10.1021/am2014103>.
 28. Liang JJ, Liao CL, Liao JT, Lee YL, Lin YL. 2009. A Japanese encephalitis virus vaccine candidate strain is attenuated by decreasing its interferon antagonistic ability. *Vaccine* 27:2746–2754. <http://dx.doi.org/10.1016/j.vaccine.2009.03.007>.
 29. Lin YL, Liao CL, Chen LK, Yeh CT, Liu CI, Ma SH, Huang YY, Huang YL, Kao CL, King CC. 1998. Study of dengue virus infection in SCID mice engrafted with human K562 cells. *J. Virol.* 72:9729–9737.
 30. Chen LK, Liao CL, Lin CG, Lai SC, Liu CI, Ma SH, Huang YY, Lin YL. 1996. Persistence of Japanese encephalitis virus is associated with abnormal expression of the nonstructural protein NS1 in host cells. *Virology* 217:220–229. <http://dx.doi.org/10.1006/viro.1996.0109>.
 31. Liang JJ, Yu CY, Liao CL, Lin YL. 2011. Vimentin binding is critical for infection by the virulent strain of Japanese encephalitis virus. *Cell. Microbiol.* 13:1358–1370. <http://dx.doi.org/10.1111/j.1462-5822.2011.01624.x>.
 32. Durbin JE, Hackenmiller R, Simon MC, Levy DE. 1996. Targeted disruption of the mouse Stat1 gene results in compromised innate immunity to viral disease. *Cell* 84:443–450. [http://dx.doi.org/10.1016/S0092-8674\(00\)81289-1](http://dx.doi.org/10.1016/S0092-8674(00)81289-1).
 33. Chen LK, Lin YL, Liao CL, Lin CG, Huang YL, Yeh CT, Lai SC, Jan JT, Chin C. 1996. Generation and characterization of organ-tropism mutants of Japanese encephalitis virus in vivo and in vitro. *Virology* 223:79–88. <http://dx.doi.org/10.1006/viro.1996.0457>.
 34. Hase T, Dubois DR, Summers PL. 1990. Comparative study of mouse brains infected with Japanese encephalitis virus by intracerebral or intraperitoneal inoculation. *Int. J. Exp. Pathol.* 71:857–869.
 35. Tu YC, Yu CY, Liang JJ, Lin E, Liao CL, Lin YL. 2012. Blocking double-stranded RNA-activated protein kinase PKR by Japanese encephalitis virus nonstructural protein 2A. *J. Virol.* 86:10347–10358. <http://dx.doi.org/10.1128/JVI.00525-12>.
 36. Kimura T, Sasaki M, Okumura M, Kim E, Sawa H. 2010. Flavivirus encephalitis: pathological aspects of mouse and other animal models. *Vet. Pathol.* 47:806–818. <http://dx.doi.org/10.1177/0300985810372507>.
 37. Wu SF, Lee CJ, Liao CL, Dwek RA, Zitzmann N, Lin YL. 2002. Antiviral effects of an iminosugar derivative on flavivirus infections. *J. Virol.* 76: 3596–3604. <http://dx.doi.org/10.1128/JVI.76.8.3596-3604.2002>.
 38. Yauch LE, Shrestha S. 2008. Mouse models of dengue virus infection and disease. *Antiviral Res.* 80:87–93. <http://dx.doi.org/10.1016/j.antiviral.2008.06.010>.
 39. Chen ST, Lin YL, Huang MT, Wu MF, Cheng SC, Lei HY, Lee CK, Chiou TW, Wong CH, Hsieh SL. 2008. CLEC5A is critical for dengue-virus-induced lethal disease. *Nature* 453:672–676. <http://dx.doi.org/10.1038/nature07013>.
 40. Tseng HJ, Lin JJ, Ho TT, Tseng SM, Hsu SH. 2011. The biocompatibility and antimicrobial activity of nanocomposites from polyurethane and nano silicate platelets. *J. Biomed. Mater. Res. A* 99:192–202. <http://dx.doi.org/10.1002/jbm.a.33175>.
 41. Piret J, Desormeaux A, Bergeron MG. 2002. Sodium lauryl sulfate, a microbicide effective against enveloped and nonenveloped viruses. *Curr. Drug Targets* 3:17–30. <http://dx.doi.org/10.2174/1389450023348037>.
 42. Decker H, Ryan M, Jaenicke E, Terwilliger N. 2001. SDS-induced phenoloxidase activity of hemocyanins from *Limulus polyphemus*, *Eurytelma californicum*, and *Cancer magister*. *J. Biol. Chem.* 276:17796–17799. <http://dx.doi.org/10.1074/jbc.M010436200>.
 43. Hellstern P, Solheim BG. 2011. The use of solvent/detergent treatment in pathogen reduction of plasma. *Transfus. Med. Hemother.* 38:65–70. <http://dx.doi.org/10.1159/000323552>.
 44. Lin YL, Lei HY, Wen YY, Luh TY, Chou CK, Liu HS. 2000. Light-independent inactivation of dengue-2 virus by carboxyfullerene C3 isomer. *Virology* 275:258–262. <http://dx.doi.org/10.1006/viro.2000.0490>.
 45. Lindenbach BD, Thiel H-J, Rice CM. 2007. Flaviviridae: the viruses and their replication, p 1101–1152. *In* Knipe DM, Howley PM (ed), *Fields virology*, 5th ed, vol 1. Lippincott Williams & Wilkins, Philadelphia, PA.
 46. Su CM, Liao CL, Lee YL, Lin YL. 2001. Highly sulfated forms of heparin sulfate are involved in Japanese encephalitis virus infection. *Virology* 286: 206–215. <http://dx.doi.org/10.1006/viro.2001.0986>.
 47. Chen Y, Maguire T, Hileman RE, Fromm JR, Esko JD, Linhardt RJ, Marks RM. 1997. Dengue virus infectivity depends on envelope protein

- binding to target cell heparan sulfate. *Nat. Med.* 3:866–871. <http://dx.doi.org/10.1038/nm0897-866>.
48. Luo M. 2012. Influenza virus entry. *Adv. Exp. Med. Biol.* 726:201–221. http://dx.doi.org/10.1007/978-1-4614-0980-9_9.
49. Nicholls JM, Chan RW, Russell RJ, Air GM, Peiris JS. 2008. Evolving complexities of influenza virus and its receptors. *Trends Microbiol.* 16: 149–157. <http://dx.doi.org/10.1016/j.tim.2008.01.008>.
50. Walsh MG. 2012. The role of hydrogeography and climate in the landscape epidemiology of West Nile virus in New York State from 2000 to 2010. *PLoS One* 7:e30620. <http://dx.doi.org/10.1371/journal.pone.0030620>.
51. Hurt AC, Chotpitayasunondh T, Cox NJ, Daniels R, Fry AM, Gubareva LV, Hayden FG, Hui DS, Hungnes O, Lackenby A, Lim W, Meijer A, Penn C, Tashiro M, Uyeki TM, Zambon M. 2012. Antiviral resistance during the 2009 influenza A H1N1 pandemic: public health, laboratory, and clinical perspectives. *Lancet Infect. Dis.* 12:240–248. [http://dx.doi.org/10.1016/S1473-3099\(11\)70318-8](http://dx.doi.org/10.1016/S1473-3099(11)70318-8).

利農力